

Mechanistic Modeling of the Impedance Response of Cathodic Reduction of Hydrogen Ion in Strong Acidic Environments

Negar Moradighadi, Yoon-Seok Choi and Srdjan Nesic

Institute for Corrosion and Multiphase Technology
Department of Chemical & Biomolecular Engineering, Ohio University
Athens, OH 45701

ABSTRACT

Studying the mechanism of electrochemical reactions benefits from implementation of steady state and transient techniques such as electrochemical impedance spectroscopy (EIS). To develop an understanding of experimental results and how they relate to corrosion mechanisms requires their comparison with a mechanistic model. In this study, a physico-chemical model was used to simulate both the steady state potentiodynamic sweep, and the EIS response of cathodic reduction of H^+ in an acidic environment. The modeled steady state potentiodynamic sweep, Nyquist plot and Bode plot were validated by comparison with experimental data.

INTRODUCTION

EIS is one of the techniques which is frequently used for studying electrochemical reactions on a metal surface in an aqueous environment. However, one of the main challenges in using EIS is the interpretation of results. Various interpretation methods and their associated uncertainties lead to ambiguous outcomes and often end up with a biased analysis. One of the methods frequently used is the so-called “equivalent electrical circuit” method which models the response of an electrochemical system by matching it to that of a combination of “analogous” electrical circuit components, such as resistors, inductors, capacitors, etc.^{1,2} However, it is often seen that several different equivalent electrical circuits match the impedance response of an electrochemical system and therefore, the analysis of the results using this approach can be misguided and ambiguous¹. Furthermore, it is not always easy to assign physical meaning to all the various electrical components of an equivalent circuit that seems to match the electrochemical data best.

Therefore, the main motivation of the present work is to directly model the impedance response of an electrochemical system by directly building a model involving electrochemical reactions and other associated processes such as mass transfer, chemical reactions, etc.^{3,4}

Consequently, the simulated impedance response using this type of model can be directly used to analyze the experimental results and evaluate mechanisms of electrochemical reactions in a complex system. In this work, the transient electrochemical/physico-chemical models behind the mechanistic corrosion prediction package MULTICORP™, have been used as a base for building a new module, LABCORP-ACT™, focused modeling the current response to an imposed alternating potential perturbation in an electrochemical system³. The physico-chemical, mathematical, and numerical aspects of this model are explained in detail in a previous paper⁵. The model describes the main reactions and processes in an electrochemical system such as electrochemical and chemical reactions at the steel surface, transport of species between the steel surface and the bulk solution, and formation/growth of corrosion product layers. All these mechanistic features make this particular model a suitable tool for simulating the impedance response of electrochemical reactions associated with the corrosion of mild steel.

RESULT AND DISCUSSION

Modeling Steady State Potentiodynamic Sweep

As the first step, the modeling of the steady state potentiodynamic sweep is required in order to establish whether the model can properly generate the steady state sweeps which would enable us to choose the desired DC potential at which the impedance response will be simulated. In an experiment, generating a potentiodynamic sweep initially requires waiting for the concentrations of the ions to get established near the metal surface in order to obtain a constant open circuit potential (OCP). Similarly, when the simulation is started it takes a certain amount of time to obtain a constant OCP.

Table 1 shows the simulation parameters for generating a steady state potentiodynamic sweep. The velocity in the simulation is the superficial velocity in a pipe with 0.1 m internal diameter, 0.02 m thickness, 20 µm roughness and conductivity of 60 W/m.K. The model was modified to output the open circuit potential at a specified time step (0.01 sec). Consequently, as shown in Figure 1, it only required about 0.1 sec to establish a stable OCP in the simulation.

Table 1. Simulation parameters for generating steady state potentiodynamic sweep.

Parameters	Values
pN ₂	1 bar (de-aerated environment)
Temperature	30°C
pH	4
Electrolyte	0.1 M NaCl
velocity	2.6 m/s

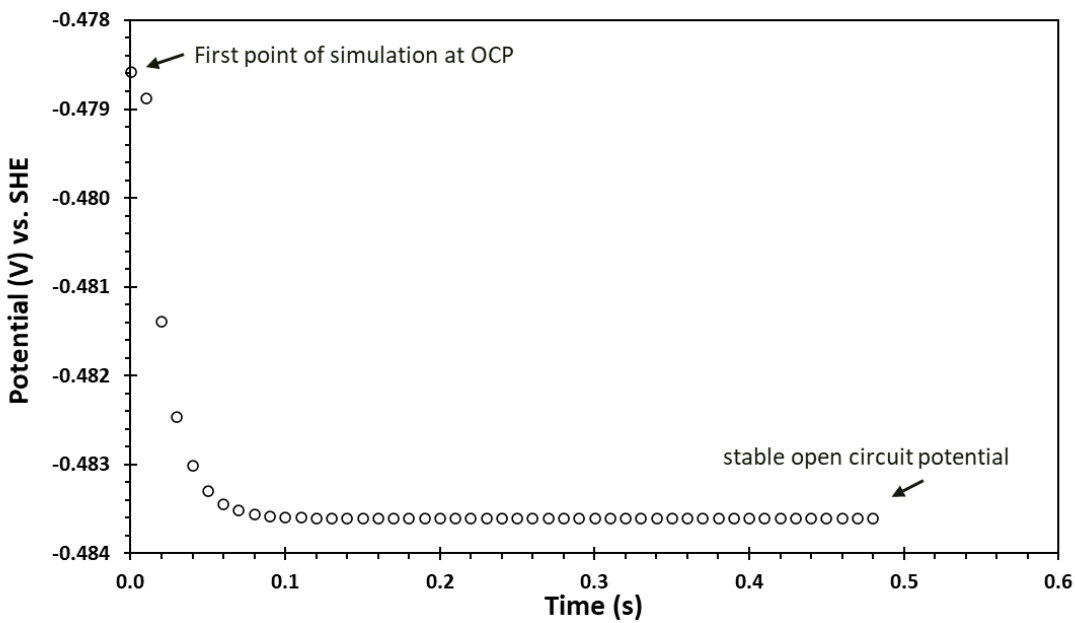


Figure 1: Calculated open circuit potential using 0.01 s time step. Simulation parameters: $pN_2= 1$ bar, pH 4, $T=30^\circ\text{C}$, velocity=2.6 m/s, 0.1 M NaCl.

After obtaining a stable OCP, the potential in the simulation was changed in the cathodic direction from OCP using a -1 mV/s sweep rate (Figure 2a) and the corresponding current density was calculated, as shown in Figure 2b. It is important to note that the chosen sweep rate was small enough to obtain a steady state current density at each potential step before changing the potential. Figure 3 shows the current density response to the first potential perturbation from the OCP ($E= -1$ mV vs. OCP). The result shows that the current density reached steady state in less than 1 s. Therefore, this analysis confirms that the potential sweep rate of -1 mV/s was acceptable for generating the steady state potentiodynamic sweep.

Both the cathodic sweep (H^+ evolution) and the anodic sweep (dissolution of iron) were generated. By summation of the anodic current density and cathodic current density, the steady state potentiodynamic sweep was obtained as shown in Figure 4.

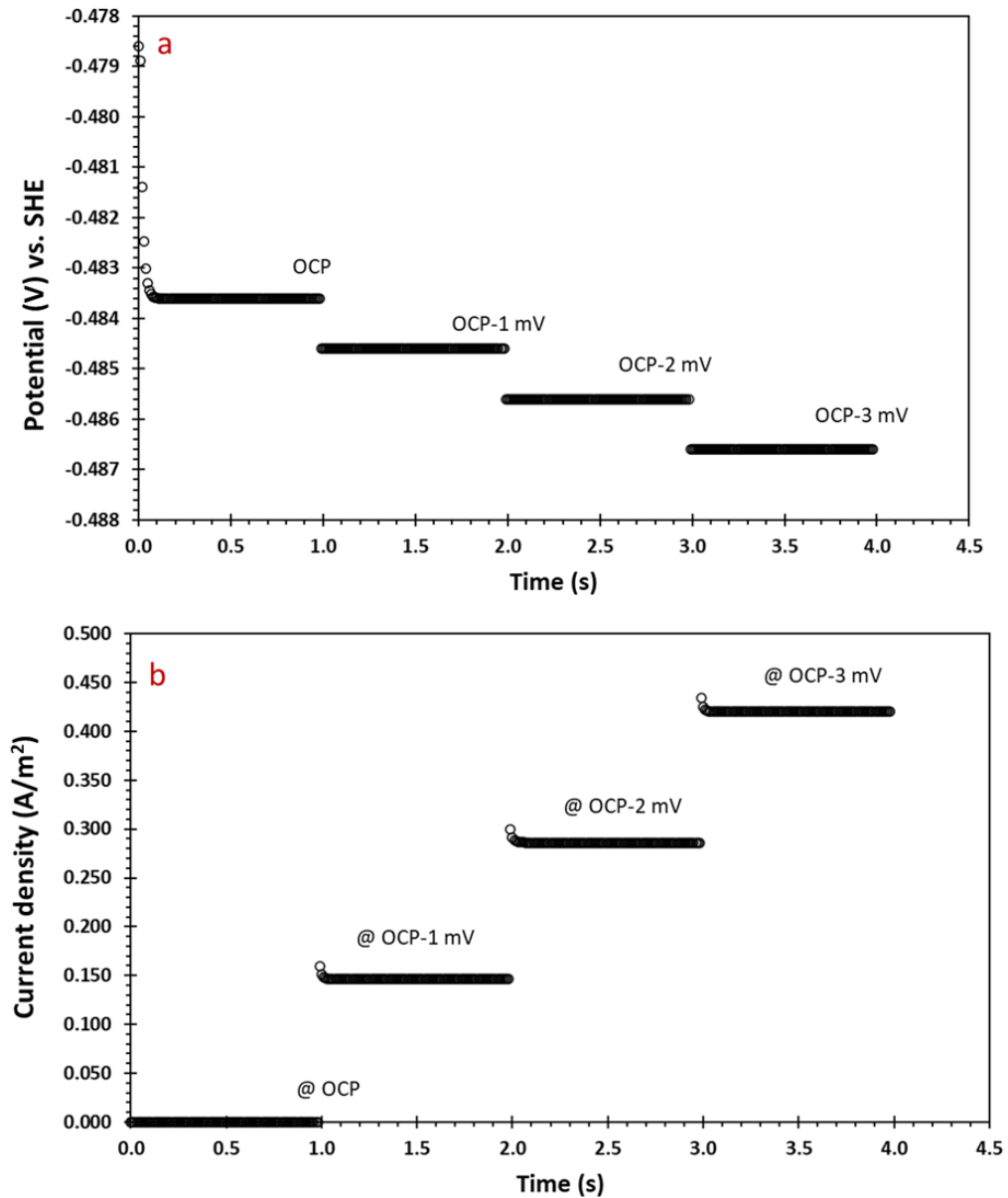


Figure 2: (a) Response when changing the potential from OCP using -1 mV/s sweep rate. (b) Current density response to each potential step. Simulation parameters: $p\text{N}_2=1$ bar, pH 4, $T=30^\circ\text{C}$, velocity=2.6 m/s, 0.1 M NaCl

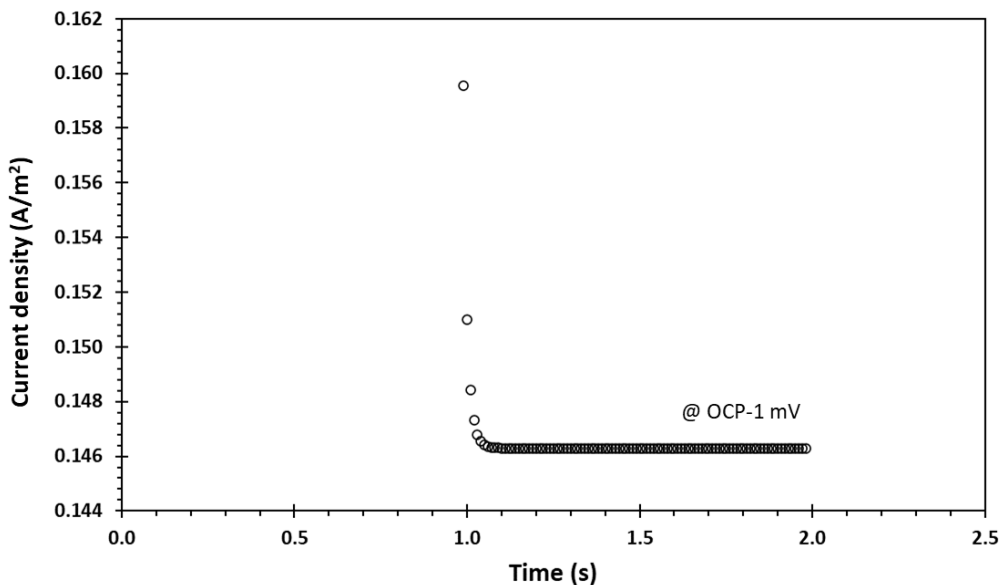


Figure 3: Calculated current density at first potential step from OCP. Simulation parameters: $pN_2= 1$ bar, pH 4, $T=30^\circ\text{C}$, velocity=2.6 m/s, 0.1 M NaCl.

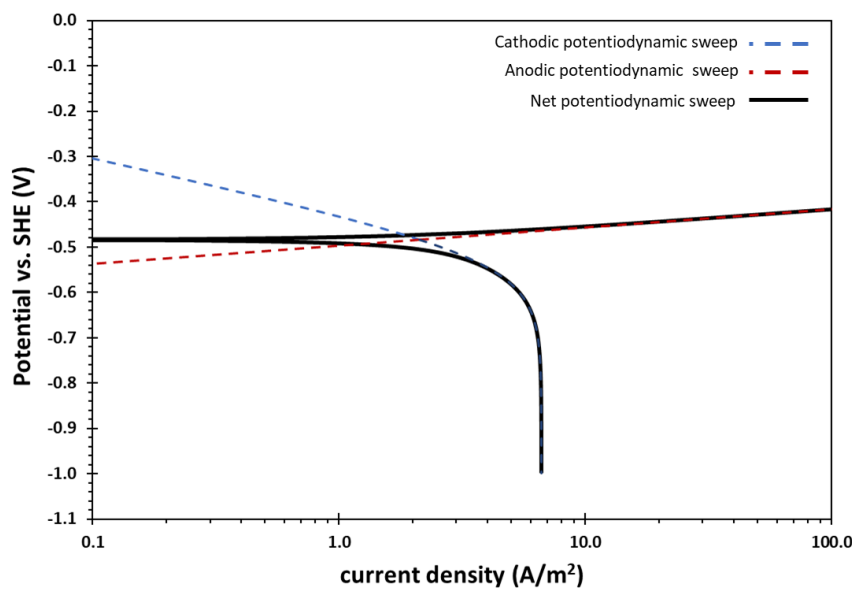


Figure 4: Calculated steady state potentiodynamic sweep. The black line represents the net current density. Simulation parameters: $pN_2= 1$ bar, pH 4, $T=30^\circ\text{C}$, velocity=2.6 m/s, 0.1 M NaCl, sweep rate =1 mV/s.

Alternative Current (AC) Response to the Imposed Alternating Potential

In the previous section, it was described how the potential was changed linearly using a specific sweep rate, and the corresponding steady state current densities were calculated. The same approach was implemented to perturb the potential in the sinusoidal form at 10 Hz frequency (f)

at 95 mV below the OCP where the impedance response is mainly related to the cathodic reaction, using Equation(1)¹.The imposed alternating potential is shown in Figure 5.

$$E = \bar{E}_{DC} + |\Delta E| \cos(\omega t) \quad (1)$$

$$i_T = \bar{i}_F + \Delta i_F \cos(\omega t) - C_{dl} |\Delta E| \omega \sin(\omega t) \quad (2)$$

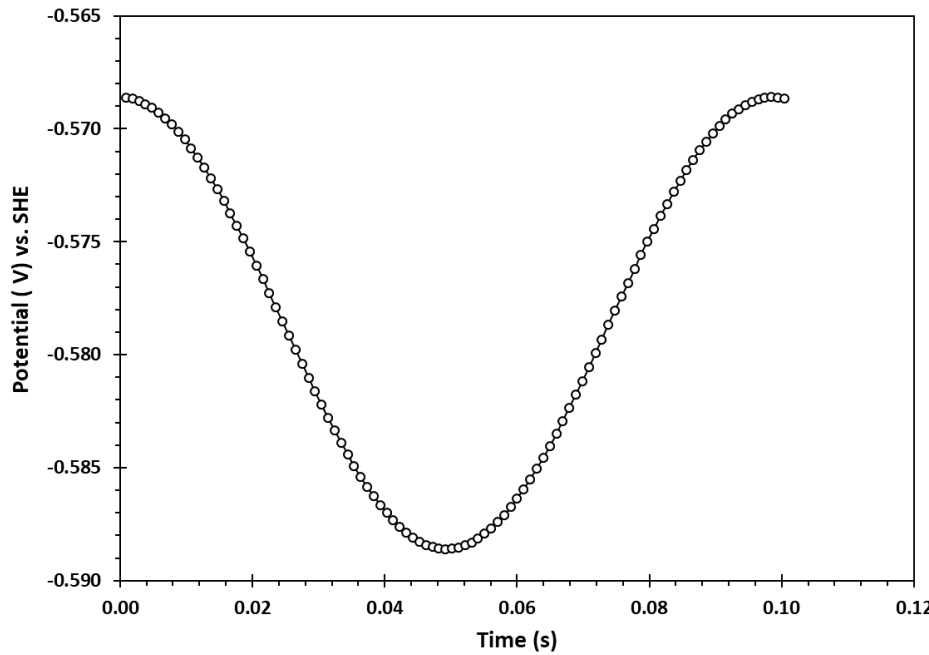


Figure 5. Imposed alternating potential using Equation (1). Simulation parameters: \bar{E}_{DC} =OCP-95 mV, $|\Delta E|= \pm 10$ mV, $f=10$ Hz, $pN_2= 1$ bar = 0, pH 4, T=30 °C, velocity=2.6 m/s, 0.1 M NaCl.

When there is a sinusoidal perturbation in potential, the responding current density originates from the electrochemical reactions (Faradaic current) as well as the double layer (charging current) at the metal surface. The current originating from the double layer is generally modeled using capacitive charge and discharge time constants. As an example, the double layer capacitance was chosen as 50 $\mu\text{F}/\text{cm}^2$ based on values reported in literature¹. As the potential was varied (Figure 5), the Faradic current density and double layer charging current density were calculated and summed according to Equation (2)¹ to obtain the total current density response as shown in Figure 6.

Once the current response to the alternating potential was obtained, the impedance was calculated using the maximum current density and the maximum perturbed potential from Equation (3)¹ and the Lissajous plot was produced, which is shown in Figure 7.

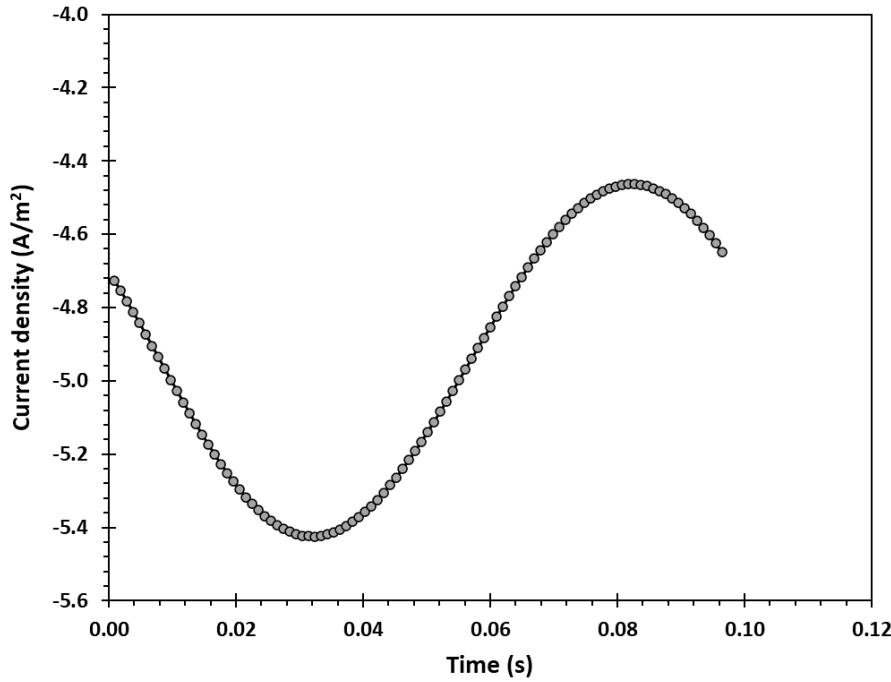


Figure 6: Calculated alternating current density using Equation (2). Simulation parameters: \bar{E}_{DC} = OCP-95 mV, $|\Delta E|=\pm 10$ mV, $f=10$ Hz, $C_{dl}= 50 \mu\text{F/cm}^2$, $pN_2= 1$ bar, pH 4, $T=30$ °C, velocity=2.6 m/s, 0.1 M NaCl.

Impedance is a complex value as the total current density lags the imposed potential. The analysis of the impedance response is based on the real (Z_r) and imaginary (Z_j) parts which are obtained using Equations (4) and (5)¹. As shown in Equations (4) and (5), the real and imaginary part of the impedance depends on phase shift (φ) between the current density and the potential. Therefore, phase shift was calculated using Equation (6) or Equation (7)¹, where the time difference is considered between the two minimum peaks in the imposed alternating potential and the obtained current shown in Figure 5 and Figure 6.

$$Z_0 = \frac{|OA|}{|OB|} \quad (3)$$

$$Z_r = Z_0 \cos(\varphi) \quad (4)$$

$$Z_j = Z_0 \sin(\varphi) \quad (5)$$

$$\varphi = \sin^{-1}\left(-\frac{OD}{OA}\right) \quad (6)$$

$$\varphi = (t_{\varphi_V} - t_{\varphi_I})2\pi f \quad (7)$$

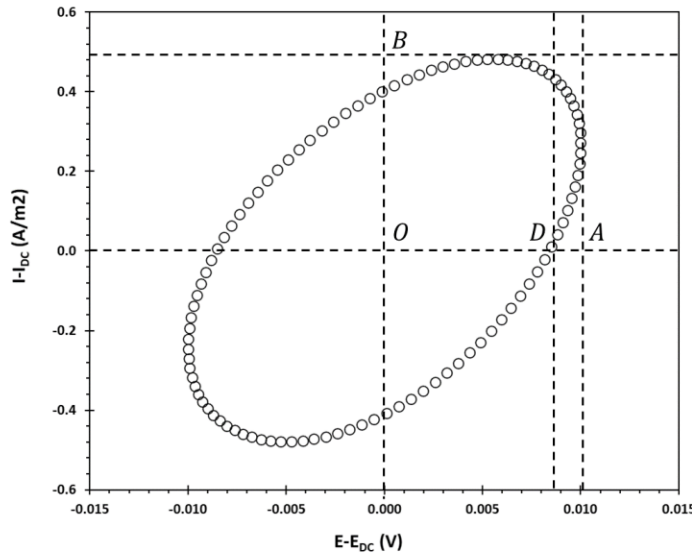


Figure 7: Modeled Lissajous plot using the data shown in Figure 5 and Figure 6 at 10 Hz frequency.

Effect of Double Layer Capacitance on the Simulated Impedance Behavior of Cathodic Reaction

To study and model the cathodic reduction of H^+ , the DC potential was chosen to be 95 mV below the OCP (at $0.75 i_{lim}$), where the current density is under mixed charge transfer and mass transfer control. At this potential, the electrochemical system can be modeled with a very simple Randles electrical circuit shown in Figure 8, in which the charge transfer resistance (R_{ct}) is in series with the diffusion impedance (Z_D) and all in parallel to the double layer capacitance (C_{dl}). Since a solution resistance (R_s) would be unnecessary in a computer simulation, this value was not used for the Randles circuit.

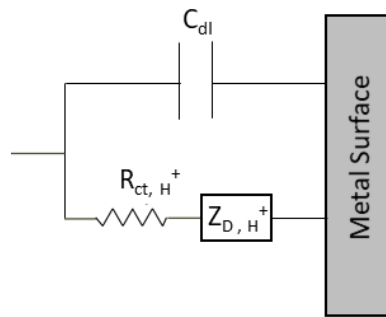


Figure 8: Equivalent electrical circuit corresponding to the electrochemical system used in this study.

Figure 10 and Figure 10 show the Nyquist plot and Bode plot of only the cathodic reaction (without the effect of double layer capacitance) in the blue solid-color markers. The impedance responses of the cathodic reaction were calculated in the frequency range of 10 kHz to 1 Hz.

In the Nyquist plot, the impedance response at the highest frequency corresponds to the charge transfer resistance (R_{ct}) of the cathodic reaction while the diameter of the Nyquist plot is related to the diffusion resistance (R_{diff}). The polarization resistance (R_p) in this case of study is the summation of the charge transfer resistance and the diffusion resistance.

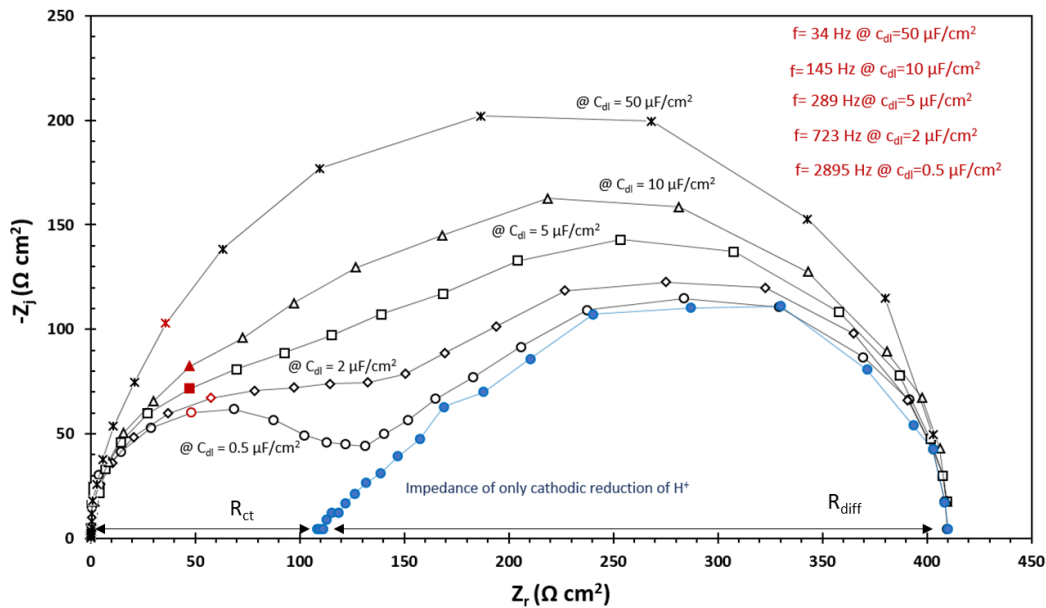


Figure 9. Diffusion impedance of the cathodic reaction and the effect of different values of the double layer capacitance on the Nyquist plot. Simulation parameters: \bar{E}_{DC} = OCP-95 mV, $|\Delta E|=\pm 10$ mV, pN₂= 1 bar, pH 4, T=30°C, velocity=2.6 m/s, 0.1 M NaCl.

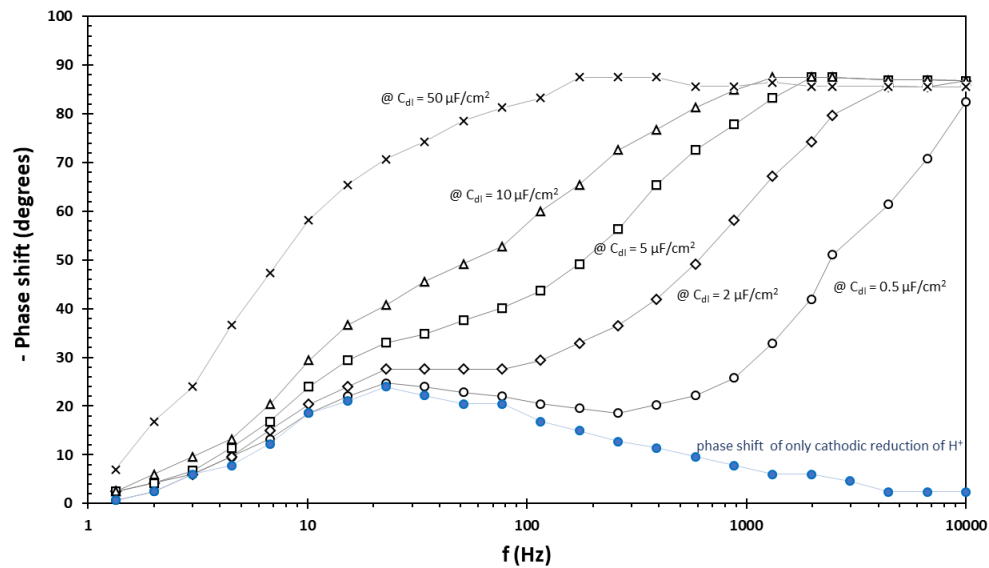


Figure 10. Bode plot of the of the cathodic reaction and the effect of different values of the double layer capacitance on the Bode plot. Simulation parameters: \bar{E}_{DC} = OCP-95 mV, $|\Delta E|=\pm 10$ mV, pN₂= 1 bar, pH 4, T=30°C, velocity=2.6 m/s, 0.1 M NaCl

Figure 9 also shows the effect of the double layer capacitance values on the impedance response of the cathodic reaction when the charging current density of the double layer is added to the Faradaic current density. When the C_{dl} decreases from 50 to 0.5 $\mu\text{F}/\text{cm}^2$, the two-time constants related to the diffusion impedance and the double layer capacitance can be distinguished. The two-time constant is clearly observed in Nyquist plot and Bode plot when the C_{dl} is equal to 0.5 $\mu\text{F}/\text{cm}^2$. The high frequency time constant is related to the double layer capacitance and the low frequency time constant is related to the diffusion impedance.

Since the impedance of the double layer capacitance and the diffusion impedance are in parallel, the impedance with the lowest value has the largest contribution to the overall impedance⁶. As shown in Equation (8), the impedance response of the double layer has an inverse relationship with its capacitance value. As the value of the capacitance increases, its impedance decreases. Consequently, the contribution of the double layer capacitance to the overall impedance increases compared to the diffusion impedance. Therefore, as the value of the double layer capacitance increases, it is harder to distinguish the two described time constants.

$$Z_C = \frac{1}{j\omega C_{dl}} \quad (8)$$

Effect of Velocity on the Simulated Impedance Behavior of Cathodic Reaction

Figure 11 shows the effect of velocity on the impedance response of only cathodic reaction (without the influence of the double layer capacitance). The chosen DC potential for the simulation is set at -240 mV vs. OCP, which is in the limiting current region as shown in Figure 4. As the velocity was increased from 1 m/s to 10 m/s, the diameter of the diffusion impedance decreases as expected. This behavior can be explained by considering the effect of mass transfer. In the limiting current region, the current density is controlled by mass transfer of H^+ from the bulk solution to the metal surface, so increasing the velocity increases the mass transfer which reduces the diffusion impedance.

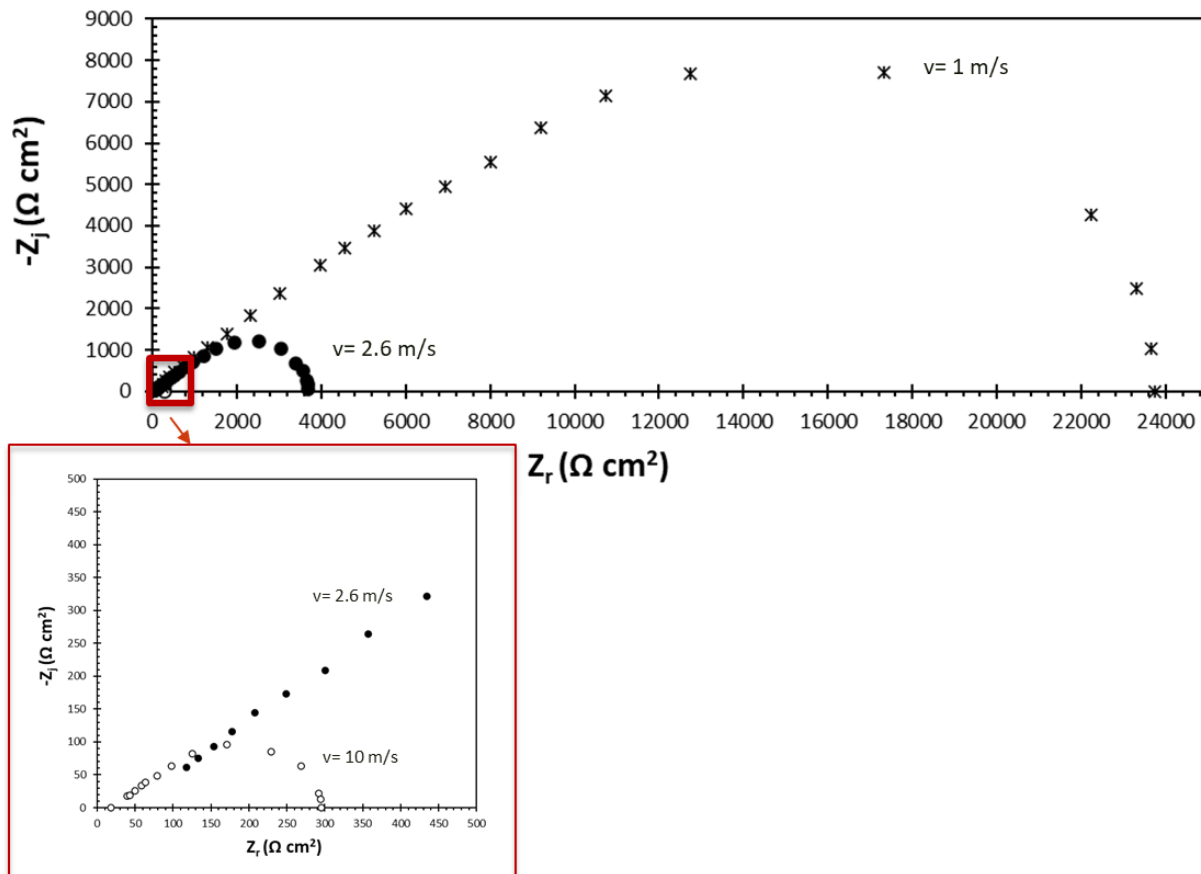


Figure 11: Effect of velocity of the diffusion impedance of the cathodic reaction.
Modeling parameters: Simulation parameters: \bar{E}_{DC} = OCP-240 mV, $|\Delta E|=\pm 10$ mV, $pN_2= 1$ bar = 0, pH 4, T=30 °C, 0.1 M NaCl.

Effect of Direct Current (DC) Potential on the Simulated Impedance Behavior of Cathodic Reaction

In the next step, the impedance response of the cathodic reaction was examined at different DC potentials. Four different potential values were selected as shown in Figure 12: +18 mV vs. OCP (at 0.25 i_{lim}), -39 mV vs. OCP (at 0.5 i_{lim}), -95 mV vs. OCP (at 0.75 i_{lim}), and -240 mV vs. OCP (virtually at i_{lim}).

Impedance responses of the cathodic reaction at these different potentials are shown in Figure 13. As potential becomes more negative, toward the limiting current density, the diameter of the diffusion impedance increases.

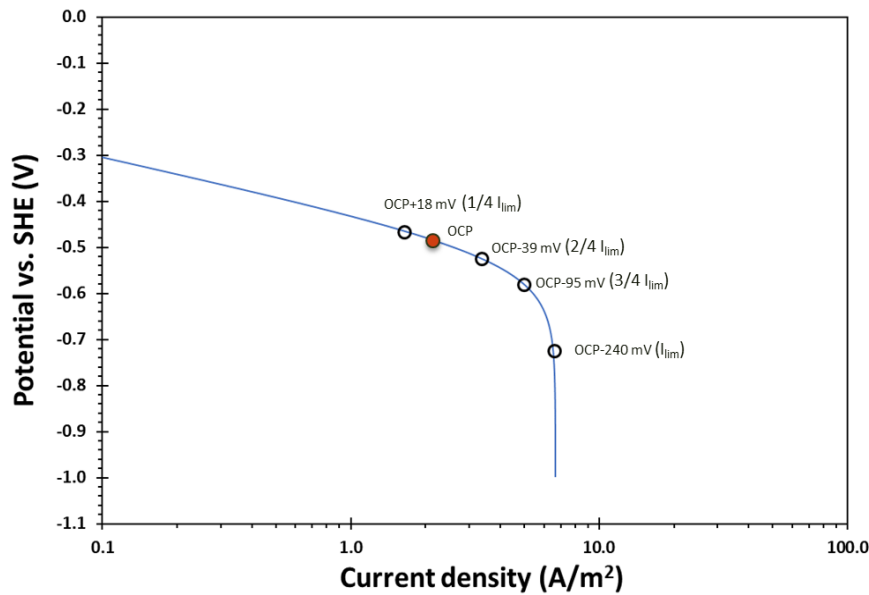


Figure 12: Steady state potentiodynamic sweep of cathodic reduction of H^+ . The points on the sweep show the DC potential for calculation of impedances shown in Figure 13.

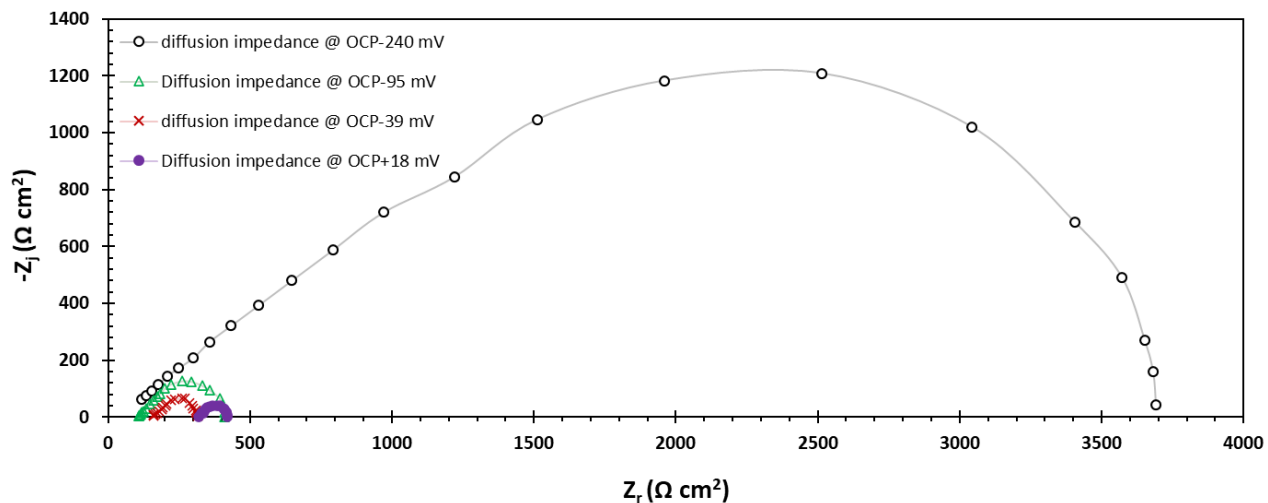


Figure 13: Nyquist plots showing the large change in diffusion impedance for the cathodic reduction of H^+ at OCP+18mV, OCP-39mV, OCP-95mV, & OCP-240mV.

Figure 14 shows the change in the charge transfer resistance, diffusion resistance and polarization resistance predicted by the impedance response of the cathodic reaction shown in Figure 13. Notice that charge transfer resistance (R_{ct}) decreases from OCP+18mV to OCP-95mV, but then remains approximately constant. In fact, the cathodic reduction of H^+ depends on both potential and surface concentration of H^+ . Therefore, at limiting current density, in which the concentration of the hydrogen ion is approximately constant, the charge transfer resistance also has a constant value. In contrast, as the potential reaches the limiting current density region, the diffusion resistance and polarization resistance keep increasing. This behavior is consistent with the experimental results and analysis reported in the literature⁷.

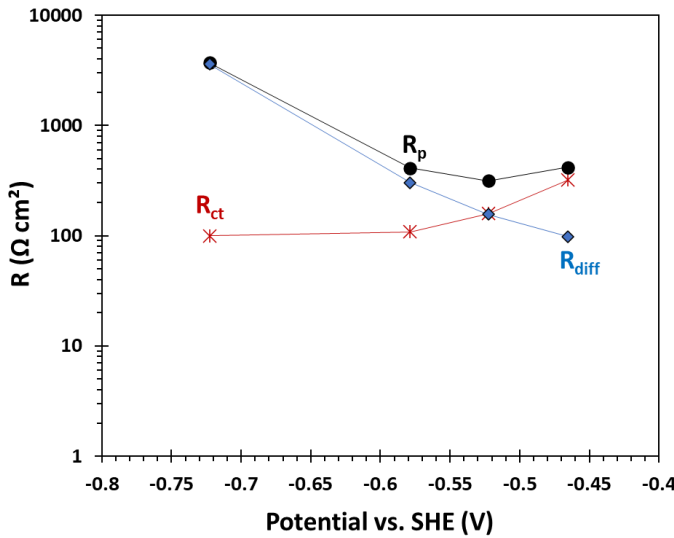


Figure 14: Values of charge transfer resistance (R_{ct}), diffusion resistance (R_{diff}) and polarization resistance (R_p) for the cathodic reduction of H^+ at OCP+18mV, OCP-39mV, OCP-95mV, & OCP-240mV.

Model Validation with Experimental Data

Experiments were performed to validate the simulated impedance response of the reduction of H^+ . Table 2 shows the simulation parameters and the experimental test conditions.

Table 2. Modeling and experimental parameters for steady state potentiodynamic sweeps and EIS.

Parameters	Values	
Test apparatus	Rotating disk electrode (RDE), three-electrode glass cell	
Sparged gas	$pN_2 = 1$ bar	
Temperature	30 ± 0.5 °C	
pH	3.00 ± 0.01	
E_{DC}	OCP-250 mV at 1000 rpm	
	OCP-290 mV at 2000 rpm	
	OCP-290 mV at 3000 rpm	
Supporting electrolyte	0.1 M NaCl	
Electrode material	API 5L X65	
Frequency	10000 to 0.01 Hz	
AC potential	10 mV rms	
Rotation rate/Velocity	For experiment using RDE	For simulation in a pipe ^{8,9}
	1,000 rpm	1.75 m/s
	2,000 rpm	2.61 m/s
	3,000 rpm	3.28 m/s
C_{dl} used in the simulation	80 $\mu F/cm^2$ at 1,000 rpm	
	70 $\mu F/cm^2$ at 2,000 rpm	
	80 $\mu F/cm^2$ at 3,000 rpm	

The details of the experimental procedure is described elsewhere⁶. The experiments were performed at pH 3 in which there is a wider range of potential for studying the impedance of the cathodic reaction as shown elsewhere⁶.

Figure 15 shows the comparison between the experimental and simulated potentiodynamic sweeps. Both anodic and cathodic reactions show a good match between experimental and simulated data at different velocities.

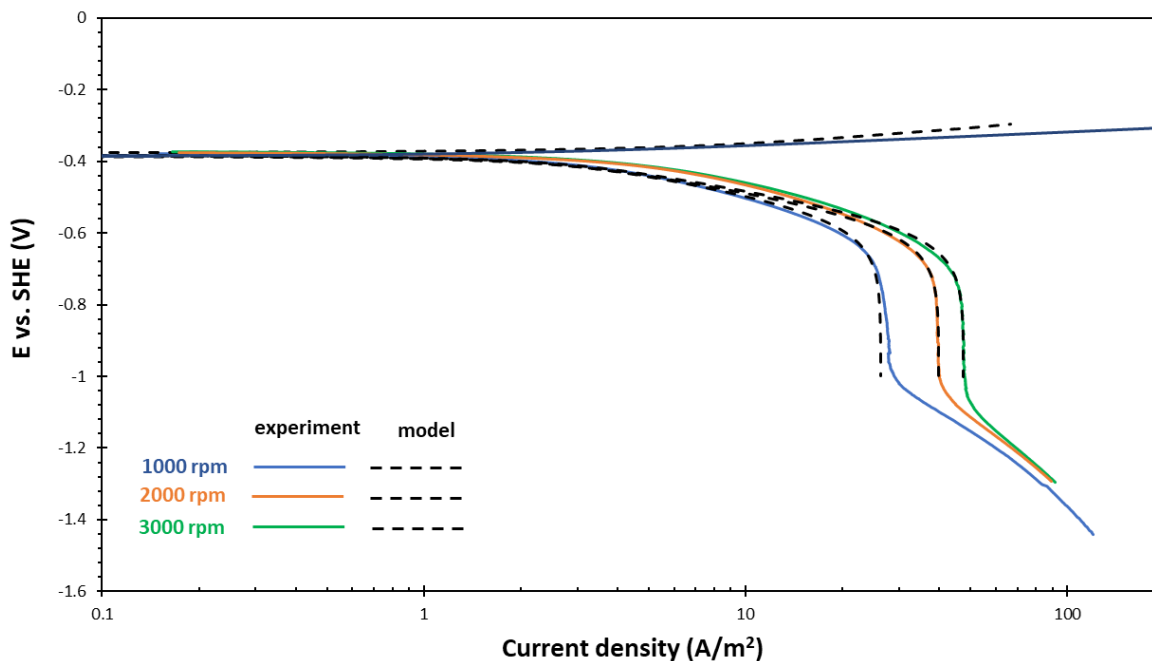


Figure 15: Comparison between the experimental and simulated steady state potentiodynamic sweep at different rotation speeds.

Figure 16 shows the comparison of the simulated and experimental Nyquist plot at different DC potentials in which the current density is approximately 80% of the limiting current density. The comparison confirms that the model predicts the impedance response of the cathodic reaction reasonably. As the velocity increases, the diameter of the low frequency time constant decreases due to the increase in the mass transfer.

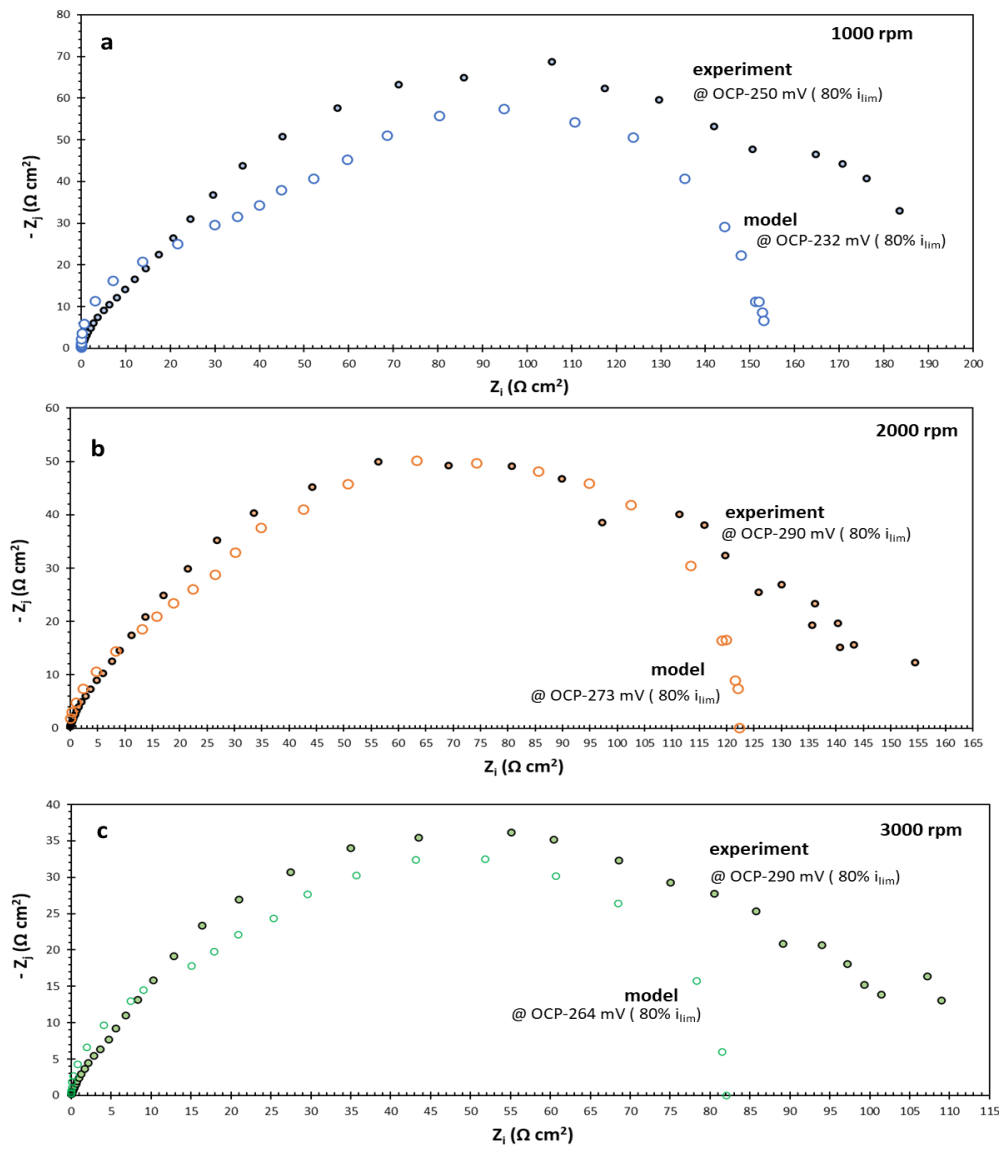


Figure 16: Comparison between the experimental and modeled Nyquist plots at different rotational rates.

CONCLUSIONS

- The impedance response, Nyquist plot and Bode plot for the cathodic reduction of hydrogen ions, were successfully modeled.
- The model prediction was in good agreement with the experimental results at different velocities and potentials.
- The model was validated by comparing the experimental and modeled data. Both potentiodynamic sweep and EIS experimental results were predicted reasonably by the model.
- The model described in this study can be used to analyze the experimental EIS results to study the cathodic reduction of the hydrogen ion related to the corrosion of the mild steel in acidic environments.

ACKNOWLEDGEMENTS

We would like to thank Dr. Bernard Tribollet for his guidance and comments in analysis of the experimental results. Moreover, the author would like to acknowledge the following companies for their financial support: Ansys, Baker Hughes, BP, Chevron, Clariant Corporation, CNOOC, ConocoPhillips, M-I SWACO (Schlumberger), Multi-Chem (Halliburton), Occidental Oil Company, Pertamina, Saudi Aramco, Shell Global Solutions, Sinclair Energy Partners, SINOPEC (China Petroleum), and TOTAL.

Appendix A. Nomenclature

C_{dl}	Double layer capacitance ($\mu\text{F}/\text{cm}^2$)
E	Electrode potential (V)
\bar{E}_{DC}	Steady state DC potential (V)
f	frequency (Hz)
i_T	Total current density (A/m^2)
\bar{i}_F	Steady state Faradaic current density (A/m^2)
i_F	Faradaic current density (A/m^2)
i_{lim}	Limiting current density (A/m^2)
j	Imaginary number ($j = \sqrt{-1}$)
R_{ct}	Charge transfer resistance ($\text{ohm}\cdot\text{cm}^2$)
R_{diff}	Diffusion resistance ($\text{ohm}\cdot\text{cm}^2$)
R_p	Polarization resistance ($\text{ohm}\cdot\text{cm}^2$)
t	time (s)
v	Velocity (m/s)
Z_0	Overall impedance (ohm cm^2)
Z_r	Real part of impedance (ohm cm^2)
Z_j	Imaginary part of impedance (ohm cm^2)

Z_C	Impedance of the double layer capacitance (ohm cm ²)
Z_D	Diffusion impedance (ohm cm ²)
ω	Angular velocity (rad/s)
φ	Phase shift (degrees)

REFERENCES

1. Orazem, M.E., and B. Tribollet, *Electrochemical Impedance Spectroscopy*, 2nd ed. (Hoboken, NJ: John Wiley & Sons, Inc., 2017).
2. Farelas, F., M. Galicia, B. Brown, S. Nesic, and H. Castaneda, *Corrosion Science* 52 (2010): pp. 509–517.
3. “MULTICORP - Corrosion Prediction Software” (n.d.), <http://www.icmt.ohio.edu/software/multicorp/multicorp%204/index.asp> (Sep. 13, 2021).
4. Harding, M., B. Tribollet, and M.E. Orazem, *Journal of The Electrochemical Society* 164 (2017): pp. E3418–E3428.
5. Nešić, S., A. Kahyarian, and Y.S. Choi, *Corrosion* 75 (2018): pp. 274–291.
6. Moradighadi, N., B. Brown, and S. Nesic, “Note on Selecting DC Potentials for EIS Measurements: An Example of Determining the Diffusion Coefficient of Hydrogen Ion in Aqueous Solutions” (OnePetro, 2021).
7. Tran, M.T.T., B. Tribollet, V. Vivier, and M.E. Orazem, *Russian Journal of Electrochemistry* 53 (2017): pp. 932–940.
8. Kahyarian, A., M. Achour, and S. Nesic, “34 - Mathematical Modeling of Uniform CO₂ Corrosion,” in Trends in Oil and Gas Corrosion Research and Technologies, ed. A.M. El-Sherik (Boston: Woodhead Publishing, 2017), pp. 805–849.
9. Silverman, D.C., *Corrosion* 55 (1999).